Journal of Plant Growth Regulation
https://doi.org/10.1007/s00344-026-12119-w

Shade-Avoidance Transcriptome Shifts and Carotenoid Depletion in *Cichorium intybus* Induced by Customized Dye-Sensitized Solar Cell Light Filtering

Fabiano Sillo[1] · Alessio Dessì[2] · Cecilia Brunetti[3] · Felicia Menicucci[3] · Sara Beltrami[4] · Elias Stathatos[5] · Gianna Reginato[2] · Raffaella Balestrini[6]

Received: 26 July 2025 / Accepted: 12 February 2026
© The Author(s) 2026

Abstract

The transition toward energy-sustainable greenhouses currently demands photovoltaic covers that can guarantee crop yield and quality by minimizing their interference with photosynthetically active radiation. Here, the impact of a novel semi-transparent dye-sensitized solar cell (DSSC) module, based on the BTD-DTP1 dye, was evaluated, considering the growth and molecular profile of radicchio plants (*Cichorium intybus* var. *latifolium* cv. Precoce). They were cultivated for 60 days under a customized-DSSC panel, clear glass, or without cover. Whole-transcriptome profiles were obtained through RNA sequencing (RNA-seq), and carotenoid and phenylpropanoid contents were analyzed. The customized-DSSC filtered light induced elongated stems and narrower leaves than the other conditions. RNA-seq data showed the upregulation of pathways associated with shade avoidance responses, including gibberellin and brassinosteroid signalling, cell-wall remodelling and nitrate transport, while photosynthesis-related ones and carotenoid biosynthesis were repressed. Consistently, neoxanthin, violaxanthin, lutein and β-carotene levels decreased in plants grown under customized-DSSC. These changes resulted from the reduced light intensity and altered light spectrum transmitted by the panel, depleted in blue and enriched in far-red wavelengths. Overall, the DSSC panel triggered the reallocation of plant resources from the photosystems toward rapid elongation, with potential consequences for crop yield. The identified molecular markers may be useful for optimizing DSSC devices and hybrid lighting strategies aimed at limiting shade-avoidance while maintaining crop productivity in agrivoltaic systems.

Keywords Agrivoltaics · RNA-seq · DSSC · Radicchio · Carotenoids · Polyphenols · Light

Communicated by Ravi Gupta.

✉ Raffaella Balestrini
raffaellamaria.balestrini@cnr.it

[1] Institute for Sustainable Plant Protection (CNR-IPSP), National Research Council of Italy, Strada delle Cacce 73, Torino 10135, Italy

[2] Institute of Chemistry of Organometallic Compounds (CNR-ICCOM), National Research Council of Italy, Via Madonna del Piano 10, Sesto Fiorentino 50019, Italy

[3] National Research Council of Italy, Institute for Sustainable Plant Protection (CNR-IPSP), Via Madonna del Piano 10, Sesto Fiorentino (FI) 50019, Italy

[4] Department of Agriculture, Food, Environment and Forestry (DAGRI), University of Florence, Viale delle Idee 30, Sesto Fiorentino, Italy

[5] BRITE Solar Technologies, Patras Science Park, GR26504, Rio-Patras, Greece

[6] Institute of Biosciences and Bioresources (CNR-IBBR), National Research Council of Italy, Via G. Amendola 165/A, Bari 70126, Italy

Published online: 03 March 2026

Introduction

Achieving high-efficiency agricultural production while minimising environmental impact has remained a central challenge for the agricultural sector. Energy stands at the heart of this challenge because almost all stages of food production require energy inputs. Pumping water for irrigation alone consumes about 1,896 PJ per year and releases roughly 216 Mt of CO_2, with groundwater lifting responsible for nearly 90% of that load (Qin et al. 2024). Greenhouses are among the most energy-intensive food-production systems because they must maintain indoor growing conditions, including temperature, humidity, and light levels, as well as a consistent photoperiod, independent of the external weather conditions. Electricity is needed for supplemental lighting, ventilation and fans, circulation pumps and fertigation, and automation processes (Trépanier et al. 2025). By harnessing real-time data monitoring, artificial intelligence, and innovative tools, the so-called "Agriculture 4.0" aims primarily to increase or maintain crop yields while shrinking this environmental footprint, leading to the creation of climate-smart farms (Dayıoğlu et al. 2021; Hahn et al. 2025; Dessì et al. 2025). In Europe, this transition is linked to the European Green Deal, which targets climate neutrality by 2050, with a particular focus on energy policy (Hainsch et al. 2022). However, innovative Agriculture 4.0 technologies, such as sensors, precision irrigation tools, climate-controlled greenhouses, require additional energy demands (Soussi et al. 2025).

In this scenario, to meet the energy requirements of the agricultural sector, current research efforts prioritise the generation and deployment of eco-efficient technologies, several of which are related to coupling renewable-energy production with farming practices (Crippa et al. 2021). One promising approach to addressing both energy demand and eco-sustainability is agrivoltaics, which integrates the generation of photovoltaic (PV) electricity with crop production to improve land-use efficiency (Barron-Gafford et al. 2019; Mazzeo et al. 2025). Light is the essential driver of photosynthetic CO_2 assimilation, supplying the energy that converts carbon dioxide into sugars. Both light quantity and spectral quality directly affect plant phenotype, also modulating the profiles and concentrations of secondary metabolites, including polyphenols and carotenoids (Loi et al. 2020). When leaves absorb sunlight, the energy follows one of three pathways: powering photochemical reactions, being re-emitted as chlorophyll fluorescence, or being dissipated as heat *via* non-photochemical quenching (Lu et al. 2024). Net photosynthesis increases with photosynthetically active radiation (PAR; 400–700 nm) from darkness up to the light-saturation point (Lu et al. 2024). Thus, both field-based agrivoltaic systems and greenhouses equipped with PV modules must balance two competing goals: allowing sufficient PAR to reach the crop by limiting shading from PV modules, and maximizing electrical yield. Conventional PV modules generally utilise opaque crystalline-silicon panels, which often shade the canopy and force a trade-off between biomass production and power output (Lu et al. 2022). Since plants absorb most PAR, but largely reflect or transmit far-red (FR) light, the light environment under a canopy exhibits a reduced red-to-far-red (R: FR) ratio (Runkle and Heins 2001), similar to what happens under a PV panel. It has been reported that perceived neighbour proximity (low R: FR) and attenuation of blue wavelengths drive petiole/axis elongation, reduced leaf expansion, and extensive transcriptional reprogramming (Fernández-Milmanda and Ballaré 2021; Pastor-Andreu et al. 2024). Low solar radiation is known to elicit the shade-avoidance syndrome (SAS) in several plant species: carbon gain and water fluxes decline, biomass accumulates in roots, stems and leaves biomass decrease, while stems and petioles elongate (Poorter et al. 2012; Wille et al. 2017).

A way to address the key drawback of opaque PV modules and to limit the effects of SAS is to develop novel devices that guarantee crop yield and quality by minimizing their interference with PAR. Semi-transparent third-generation PV technologies such as dye-sensitised solar cells (DSSCs) offer a spectral-splitting strategy (Ursu et al. 2022; Stallknecht et al. 2023). Under these devices, selected wavebands that are outside the PAR range are harvested for electricity generation, while the PAR is transmitted to the crop. By harvesting solar energy in greenhouses, these devices may simultaneously drive heat-pump and LED lighting systems while transmitting photosynthetically optimal wavebands to the crop, decreasing external energy inputs and improving the sustainability of the whole system (Lu et al. 2024). In this context, semi-transparent PVs could be integrated into façades, windows, urban structures, and greenhouses, transmitting a portion of sunlight with tunable transparency to maintain daylighting while generating power (Montes-Romero et al. 2025). In addition, the colour and semi-transparency of DSSCs can be finely customized through the choice of specific photosensitisers (Muñoz García et al. 2021; Barichello et al. 2024). The role of the dye in DSSCs is to initiate charge separation and determine which wavelengths are absorbed and which are transmitted. By selectively modifying the dye structure, it is possible to tune both the absorbed and transmitted radiation, a feature that makes DSSCs particularly suitable for agrivoltaic panels where specific spectral bands must reach the crop (La Notte et al. 2020; Lu et al. 2024). Beyond electricity generation, in greenhouses DSSCs can also reduce internal temperatures and regulate relative humidity, thus improving microclimate control (Roslan et al. 2021).

These promising spectral and microclimatic advantages have encouraged researchers to conduct greenhouse trials assessing plant responses under DSSC roofs. However, to date, studies evaluating crop responses under DSSC roofs have used commercial Ru-based dyes (e.g. Z907). These experiments were carried out on different plant species, including tomato (Ntinas et al. 2019), *Orthosiphon stamineus* (Roslan et al. 2021), coleus (Park et al. 2024) and petunia (Kim and Oh 2024). Overall, benefits such as lower canopy temperatures and faster growth in plants associated with the use of DSSCs were reported (Park et al. 2024; Kim and Oh 2024). For example, red-absorbing DSSCs reduced the daily light integral received by plants of *Petunia* × *hybrida* to approximately 45% compared to controls, decreasing the blue: red photon ratio, and resulting in stem elongation, increased leaf area, and delayed flowering, a typical response to the limitation of blue light (Kim and Oh 2024). Current optimisation of DSSC focuses on both device architecture, e.g., TiO_2 layer thickness and sealing strategies (Barichello et al. 2024), as well as dye chemistry. Dyes like thiazolo[5,4-*d*]thiazole- and dithienopyrrole-based photosensitisers, which balance plant photoreceptor sensitivity with photovoltaic performance, are attracting interest in the production of DSSC panels (Dessì et al. 2020, 2021). However, plants are known to have a high degree of plasticity in response to changes in light conditions, adjusting the organization and function of their photosynthetic apparatus accordingly, and plant responses to spectrally selective covers are reported to be species specific (Pons et al. 2004; Casal and Fankhauser 2024). Nevertheless, understanding of the molecular plant response, including transcriptomic remodelling, involved in the adaptation to PV-filtered light is still limited, and is focused on early seedling stages (Spampinato et al. 2025).

In this work, focusing on radicchio (*Cichorium intybus* var. *latifolium cv*. Precoce) as a model leafy crop, transcriptomic and biochemical changes induced by the use of a customized DSSC panel as a cover in a controlled condition experiment were assessed. Radicchio, a member of the chicory family and known for its bitter taste and high anthocyanin content, is popular in global markets and can be grown in fields or greenhouses as it is well-suited to pot cultivation due to its compact size (Bais and Ravishankar 2001). Here, radicchio plants were cultivated in a greenhouse under a new customized DSSC panel, a clear glass panel of identical size, and uncovered control. Transcriptomic profiles of the radicchio seedlings grown under the different conditions were obtained through RNA-sequencing. Additionally, carotenoids and polyphenols were characterized and quantified to decipher the molecular and biochemical response of the plants grown under these innovative PV modules.

Materials and Methods

Design, Customization and Fabrication of the DSSC Panel

A semitransparent dye-sensitized solar module of an appropriate size (Figure S1–47 × 38 cm^2 – 22 serially connected individual solar stripes – active area: 770 cm^2) was assembled in collaboration with Brite Solar Technologies (Patras, Greece) to simulate the operating conditions of a dye-sensitized photovoltaic greenhouse and properly conduct our biochemical and transcriptomic experiments on radicchio plants. BTD-DTP1 was selected as the dye (Figure S1), as its design was originally conceived for agrivoltaic applications (Dessì et al. 2021). Fine tuning of the chemical structure of the photosensitizer allowed the achievement of a dye transmittance spectrum with a sufficient degree of complementarity with the photosynthetically active radiation (PAR), as shown in Figure S1c. Moreover, the dye can be prepared in only five steps, taking advantage of a straightforward synthesis that enables the high-scale preparation necessary for the DSSC module assembly. Semitransparency of the DSSC module in the entire visible region was obtained by employing a hand-made TiO_2 paste and limiting the TiO_2 thickness to just 3 µm (determined by SEM cross section images; Figure S2). The porosity of the films was 110 m^2/g, ensuring the absorbance of a high volume of dye molecules. To reduce the risks of leaks of the electrolyte solution, minimize the sealing problems, and avoid changes in the light absorption by the panel in the course of the experiments, a quasi-solid state electrolyte was used in the construction of the DSSC module. In particular, a hybrid organic-inorganic material (ICS-PPG230), prepared according to procedures described in previous publications (Stathatos et al. 2000; Stathatos, 2005), was chosen. To ensure electrical connections between the stripes, the DSSC panel was fabricated using a sandwich Z-interconnection, in which the working electrode is deposited on one glass and the counter electrode on the second glass. The in-series interconnection is schematically illustrated in Figure S1d.

Commercially available lithium iodide, iodine, 1-methyl-3-propylimidazolium iodide, tert-butyl pyridine, guanidine thiocyanate, chloroplatinic acid hexahydrate (H_2PtCl_6), poly(propylene glycol)bis(2-aminopropyl) ether 230, 3-isocyanatopropyltriethoxysilane and all solvents were purchased from Sigma-Aldrich and used as received. SnO_2:F transparent conductive electrodes (FTO, TECTM A10) 10 Ohm/square were purchased from Pilkington NSG Group. UV-cured resin ThreeBond was used to isolate the silver grids inkjet printed on FTO glasses using Cabot silver ink. Commercial ultra-pure titanium butoxide (TTBU, 97%, Aldrich), Triton X-100 (polyethylene glycol p-tert-octylphenyl ether)

surfactant (99.8%, Fisher Scientific), and glacial acetic acid (AcOH, Aldrich) were used to make precursor TiO_2 sols.

Transparent thin TiO_2 films were fabricated by a sol-gel method following a previously reported procedure. Briefly, for a 10.8 mL solution, 1.44 g of Triton X-100 was mixed with 8 mL of EtOH, followed by addition of 0.8 mL of glacial acetic acid and 0.74 mL of titanium butoxide under vigorous stirring. After a few minutes of stirring, the solution was deposited on the FTO glasses by inkjet printing (Dimatix, Materials Printer DMP-5000). The films were calcined at 500 °C for 15 min using a 40 °C/min heating ramp rate. The procedure of sequential printing and sintering was repeated several times until the TiO_2 films were approximately 3 µm thick. BTD-DTP1 organic dye in chlorobenzene (CB) was also inkjet printed on TiO_2 (dye concentration: 10^{-2} M) in order to sensitize the TiO_2 electrode in the visible. The dye was adsorbed within 3 min of deposition. Excessive dye molecules that were not adsorbed on the TiO_2 surface were removed by rinsing the electrode with CB. The platinized FTO glasses were made by inkjet printing of an H_2PtCl_6 solution (5 mg/1 ml of *n*-propanol) followed by heating at 500 °C for 10 min.

The gel electrolyte was synthesized as follows: 1.4 g of the functionalized alkoxide precursor ICS-PPG230 was dissolved in 4.8 g of sulfolane under vigorous stirring. Then, 1.2 mL AcOH was added, followed by the addition of 0.3 M 1-methyl-3-propylimidazolium iodide (MPImI), 0.1 M LiI and 0.05 M I_2 in a final molar ratio of AcOH: LiI: MPImI: I_2 = 2.5:0.1:0.3:0.05. Finally, 0.5 M of *tert*-butyl pyridine and 8.9 mg of guanidine thiocyanate were added to the above mixture.

To fabricate the dye-sensitized solar panel, a silver paste was printed on the glasses to make the internal electrical connections and serially connect the adjacent cells. After the deposition of the silver fingers, the glasses were sintered at 400 °C for 10 min before the application of the dye and the electrolyte. A UV-curing resin was used to insulate the silver wires to avoid their corrosion from the electrolyte. Finally, a large area module with total size 47×38 cm^2 was fabricated after merging the two photoelectrodes and sealing them with the UV-cured resin ThreeBond. The electrolyte was inserted between the individual solar stripe electrodes through some holes present in the slightly platinized FTO counter electrode when it was still in liquid phase, which was finally gelled within an hour due to inorganic polymerization-condensation of the triethoxylane groups at both edges of the hybrid ICS-PPG230 material in the electrolyte.

Plant Material and Growth Conditions

To verify that the customized-DSSC filtered light does not affect seed germination, a first germination assay was performed before the main experiment in the greenhouse. Lighting was provided by 400 W high-pressure sodium (HPS) lamps delivering approximately 500 µmol m^{-2} s^{-1} PPFD at the canopy level. The lamps used were Philips SON-T Agro 400 W HPS lamps, with a spectral power distribution dominated by yellow-orange-red wavelengths (560–640 nm) and an enhanced emission in the blue region compared to standard HPS lamps, due to the addition of xenon (commercially described as the "Agro" spectrum). Specifically, 9 seeds of *Cichorium intybus* var. *latifolium cv*. Precoce (common name "radicchio", kindly provided by "La Semiorto Sementi" seed company, Sarno, Italy) were sown in $9 \times 9 \times 10$ cm pots filled with a 7:3 (v/v) peat-sand mix and placed either under the developed customized-DSSC panel, namely "DSSC" samples, under an identically positioned clear glass panel, namely "GLASS samples", and without any panel, namely "OUTSIDE" samples. The GLASS panel was a fluorine-doped tin oxide (FTO) coated glass slide, a common conductive glass substrate used for DSSC manufacturing. FTO is transparent to visible light, but absorbs UV light (Chowdhury et al. 2013). Germination was scored after 7 days. The assay was repeated four times.

For the main experiment, seeds of *C. intybus* var. *latifolium* cv. Precoce were germinated for 5 days on moist filter paper in 12 cm^2 Petri dishes in dark conditions. Uniform seedlings were then transferred to $9 \times 9 \times 10$ cm plastic pots filled with a 7:3 (v/ v) mix of commercial peat and autoclaved quartz sand. Pots were kept in a greenhouse maintained at 19–26 °C and around 55% relative humidity under a 16 h light / 8 h dark photoperiod. Lighting was provided as described above for the germination assay. Three light-filter conditions were assessed: (1) "DSSC", by using the DSSC panel positioned approximately 15 cm above the canopy using six plastic supports placed around it; (2) "GLASS", by using a clear glass panel of the same size and in the same position; and (3) "OUTSIDE", consisting of plants with no cover. For each treatment three pots were prepared, each pot containing three seedlings (n = 9 per condition). Plants were watered to field capacity every three days and received no additional fertilizer. The experiment was conducted from February 2024 to April 2024.

Sampling, RNA Extraction and RNA-seq Analysis

At 60 days after sowing, all three plants contained in each pot were harvested and pooled to create one composite sample per pot as a single biological replicate. Shoots were frozen in liquid nitrogen and stored at − 80 °C. To isolate RNA from plant material, for each biological replicate, approximately 100 mg of frozen tissue was ground with two 0.4 mm steel beads in a 2 mL tube using a TissueLyser II (Qiagen) for 60 s at 28 Hz. Total RNA was isolated with a modified CTAB protocol (Chang et al. 1993) and eluted in nuclease-free water. RNA concentration and purity were checked with a NanoDrop 2000 (Thermo Fisher Scientific). Stranded RNA-seq libraries were generated by IGA Technology Services (Udine, Italy) with the VAHTS Universal V10 RNA-Seq kit (Vazyme) following the manufacturer's instructions (fr-first-strand workflow). Libraries were sequenced on an Illumina NovaSeq 6000 platform to obtain 150 bp paired-end reads. In total, nine libraries (three per condition) were obtained. Basecalling, demultiplexing and adapter masking were carried out with Illumina BCL Convert v3.9.31. Reads were quality-trimmed with ERNE and mapped to the available *C. intybus* reference genome (Fan et al. 2022) using STAR v2.7.3a (Dobin et al. 2013) with default parameters. Transcript reconstruction and abundance estimation were performed with StringTie v2.1.7. Gene-level counts were performed with HTSeq-count v0.11.3 (union mode). Differential expression was analysed in DESeq2 v1.38.0 (Love et al. 2014) using GLASS as the reference treatment. Genes showing an adjusted p-value ≤ 0.05 were considered differentially expressed (DEGs). Both the full transcript set and the list of DEGs were annotated with Blast2GO v6.0 against the NCBI RefSeq protein database. Gene Ontology terms were assigned where possible. Raw sequencing data have been deposited in the NCBI Sequence Read Archive under BioProject accession PRJNA1293957.

To have an overview of the functional distribution of differentially expressed genes across metabolic pathways, the translated peptide sequences of *Cichorium intybus* were annotated using the Mercator4 web server (https://plabipd.de/portal/mercator4; Schwacke et al. 2019). Mercator4 assigned functional categories (BINs) to each sequence based on comparisons to multiple reference databases, including TAIR, Swiss-Prot, KEGG, and COG. The resulting mapping file was combined with the DEG expression data to produce MapMan-compatible input tables. Visualization was performed using MapMan software version 3.5.0, generating pathway overviews in which $\log_2$ fold-change values were represented by a color scale.

Characterization and Quantification of Photosynthetic Pigments

After lyophilization, about 10 mg per sample were subjected to chlorophyll and carotenoid extraction with 3 × 0.5 mL of acetone using an ultrasonic bath at 4 °C, for 20 min (Ashenafi et al. 2023). Extracts were centrifuged at 14,800 rpm for 5 min, and 200 µl of the supernatants were stored at – 80 °C for the HPLC analysis. Individual carotenoids and chlorophylls were analyzed by injecting 10 µL into the HPLC-DAD equipment described above. The pigments were separated using a 250 × 4.6 mm Zorbax SB-C18 (5 µm) column (Agilent Italia, Milan, Italy), kept at 40 °C, eluted with a linear gradient of solvent (A) CH_3CN/MeOH (97/3 v/v) and (B) MeOH/ethyl acetate (68/32 v/v). The separation was performed at in a 40-minutes run a flow rate of 0.7 mL min^{-1} following the gradient: 15 min (100% A); 15–28 min (0–100% B), 28–40 min (100% B). Ten minutes of conditioning were used to return to the initial conditions of the method. Individual pigments were identified and quantified by comparison of UV-visible spectral characteristics and retention times with those of authentic standards (lutein, zeaxanthin, chlorophyll a, chlorophyll b, and β-carotene), injected under the same chromatographic conditions. For quantification, five-point calibration curves of each standard were used. The analyses were conducted in triplicate, and the results were expressed as milligrams per gram of dry weight (mg g^{-1} DW).

Characterization and Quantification of Phenylpropanoids

After lyophilization, about 10 mg per sample were extracted with 3 × 0.5 mL of 75% ethanol solution (pH 2.5 adjusted with formic acid). The extracts were centrifuged at 14,800 rpm for 5 min, and the supernatants were partitioned with 4 × 0.5 mL of *n*-hexane to remove lipophilic compounds. The hydroethanolic phase was reduced to dryness using a centrifugal vacuum concentrator, and the residue was resuspended with 200 µL of MeOH: Milli-QH_2O solution (1/1 v/v, pH 2.5 adjusted with formic acid), centrifuged at 14,800 rpm for 5 min and analyzed by HPLC. The analyses of phenylpropanoids in the extracts were performed by injecting 15 µL aliquots into a PerkinElmer Flexar liquid chromatograph equipped with a quaternary 200Q/410 pump and an LC 200 diode array detector (DAD) (PerkinElmer, Bradford, CT, USA). Phenylpropanoids were separated by a Zorbax® C-18 column (250 mm × 4.6 mm, 5 µm particle size) operating at 40 °C. The mobile phases consisted of (A) acidified water (0.1% HCOOH) and (B) acetonitrile (0.1% HCOOH). The separation was conducted using the following gradient:

4 min (5% B); 4–24 min (3–20% B), 24–39 min (20–50% B), 39–52 min (50–100% B), 52–54 min (100-5% B) with of a total analysis time of 54 min, at a flow rate of 0.6 mL min^{-1}. Ten minutes of conditioning were used to return to the initial conditions of the method. Chromatograms were recorded at 280 nm for epigallocatechin derivatives, at 330 nm for hydroxycinnamic acids, and at 350 nm for flavonols. The identification of polyphenols in the extracts was carried out based on previous identification (Menicucci et al. 2025) and by comparing the UV-visible spectral characteristics of the peaks and the retention times with those of authentic standards (epigallocatechin, chlorogenic acid, cichoric acid and kaempferol-3-*O*-glucuronide) injected under the same conditions. For quantification, four-point calibration curves of each standard were used. The analyses were conducted in triplicate and the results were expressed as milligrams *per* grams of dry weight (mg g^{-1} DW).

Statistical Analysis

Statistical analysis was conducted with R software v. 4.3.2. After checking the normality of the distribution by Shapiro-Wilk test and homoscedasticity by Levene test of the data, one-way ANOVA was performed to assess the effects of the cover condition on carotenoid and polyphenols content. Post-hoc analysis was performed through Tukey HSD Test with a significance level set to $p \leq 0.05$. In addition, to integrate transcripts and pigments, we paired RNA-seq normalized read counts (see Table S2) with the raw carotenoid concentrations per replicate (neoxanthin, violaxanthin, lutein, zeaxanthin, β-carotene, chlorophyll a/b). Selected genes were L2E82_42560 (protochlorophyllide reductase), L2E82_36523 (chlorophyll a–b binding protein 7), L2E82_26610 (chlorophyllide a oxygenase), L2E82_06716 (carotenoid cleavage dioxygenase 4), L2E82_43989 (zeaxanthin epoxidase), L2E82_01059 (lycopene β-cyclase). Each gene was associated with the carotenoid content, and within-feature z-scores (to remove scale differences between features) across the six replicates (GLASS and DSSC samples) was determined to estimate a single pooled Pearson correlation ($n = 36$ pairs, two-sided $\alpha = 0.05$).

Results

Germination Assay and Phenotype of the Plants

Across four independent replicates, final germination percentages were 72 ± 19% under the DSSC mini-panel, 86 ± 21% beneath the glass, and 67 ± 16% with no cover (mean ± SD, $n = 4$). Pooled counts were 26/36, 31/36 and 24/36 seeds, respectively. A χ^2 test (germinated/not germinated) showed no significant effect of condition ($\chi^2 = 3.85$, df = 2, $p = 0.15$), confirming that the use of the DSSC did not significantly affect seed germination compared to glass or no cover conditions. Radicchio plants grown without cover (OUTSIDE) and under the glass panel (GLASS) showed a similar overall phenotype (not shown). Conversely, plants grown under the customized DSSC panel (Fig. 1a, b) showed reduced leaf expansion and narrower leaf blades compared to those grown under standard glass. In addition, DSSC-grown plants exhibited elongated petioles (Fig. 1b, c).

Transcriptomic Profile of Radicchio Plants Grown under Customized-DSSC and Without Cover

The RNA-seq generated an average of 35.12 million raw reads *per* sample. Reads mapping to *C. intybus* reference genome (Fan et al. 2022) resulted in an average mapping rate of 87.71% (max 88.6%, min 86.4%; Table S1-S2). The PCA of normalized read count data (Fig. 2a) showed that PC1 (53% of the total variance) separated the DSSC samples from both GLASS (reference) and OUTSIDE, indicating that the effect of the DSSC panel on transcriptomic profiles was the main source of variation. PC2 (21% of the total variance) allowed only slight separation of GLASS and OUTSIDE samples, with some overlaps (Fig. 2a). A distinct transcriptomic profile of DSSC samples compared to both OUTSIDE and GLASS samples was observed (Fig. 2b for a representative example of the top 50 most variable genes in this condition). In Fig. 2c, a Volcano plot shows the distribution of DEGs identified in DSSC and OUTSIDE conditions with respect to GLASS one. Using GLASS as reference (control), 4,161 DEGs under the DSSC panel were identified (2,014 up- and 2,147 down-regulated; adj. $p < 0.05$), while the OUTSIDE condition differed from the control only in 70 genes (21 up- and 49 down-regulated). DSSC-filtered light triggered a 90-fold larger transcriptional reprogramming than removing the cover (OUTSIDE condition), with approximately 9.5% of genes of *C. intybus* genome that were differentially expressed compared to the control condition.

Eight biological-process (BP) GO terms were significantly enriched among the up-regulated gene set (Fig. 3a). These terms were mainly related to stress and defence responses, i.e., Response to wounding (GO:0009611), Defense response (GO:0006952), Cellular oxidant detoxification (GO:0098869), Response to light stimulus (GO:0009416), together with Negative regulation of endopeptidase activity (GO:0010951). Lignin catabolic process (GO:0046274) and Nitrate transmembrane transport (GO:0015706) were also identified among enriched GO terms (Fig. 3a). On the other hand, six BP terms were over-represented in the

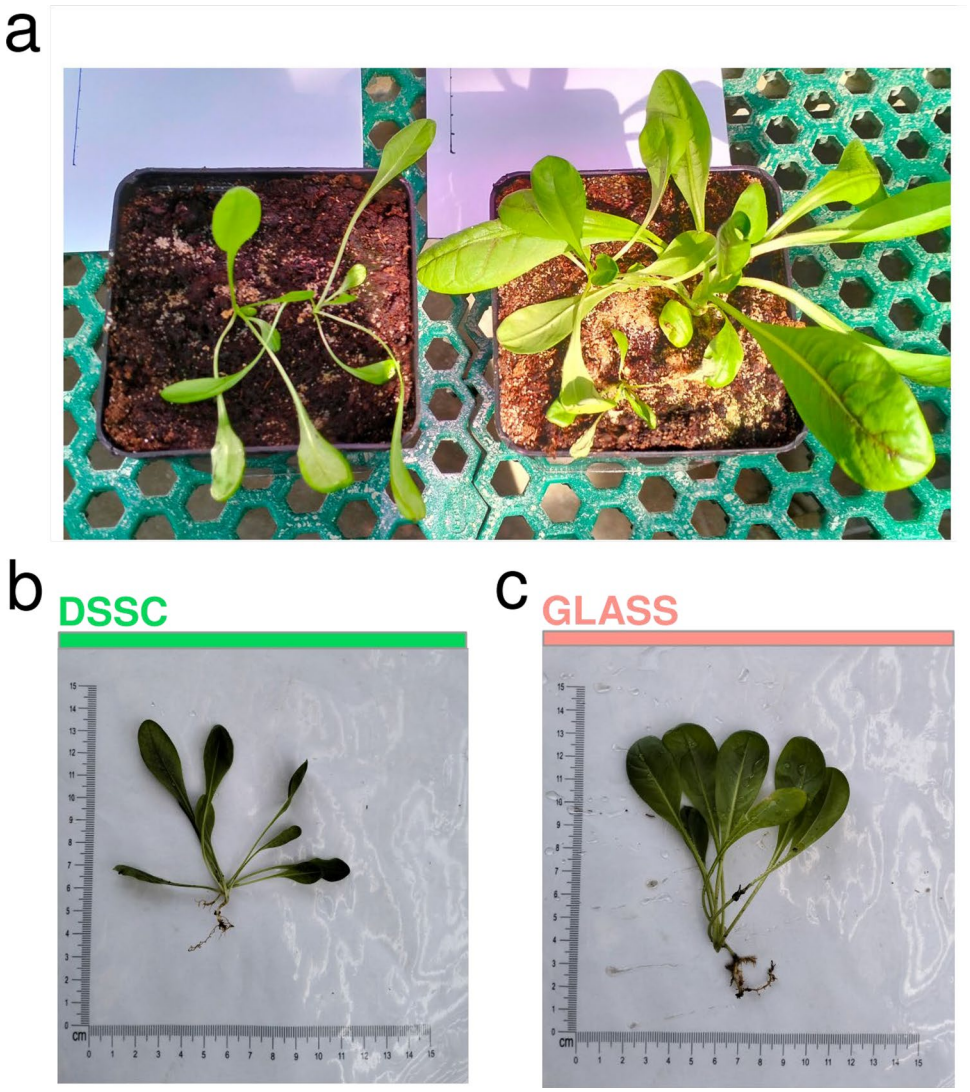


Fig. 1 Representative examples of phenotype of radicchio plants grown under the customized-DSSC panel (**a**, left; **b**) and under the glass panel (**a**, right; **c**)

down-regulated genes. The main affected process was photosynthetic capacity: the broad parent term Photosynthesis (GO:0015979) and its children terms Light harvesting in PSI/PSII (GO:0009765), Photosynthetic electron transport chain (GO:0022900), Chlorophyll biosynthetic process (GO:0015995), were identified as enriched among the down-regulated genes in DSSC samples. Additionally, Plastid organisation (GO:0009657) and Response to blue light (GO:0009637) suggested that plastids and perception of blue radiation were affected in the DSSC samples (Fig. 3a). No enriched GO terms were identified in the up- and down-regulated gene datasets of OUTSIDE samples.

Among the up-regulated genes in DSSC-grown *radicchio* plants (Table S3), several main functional groups were detected, all putatively related to shade avoidance response (Li and Wang 2022). Particularly, processes correlated with primary and secondary cell wall synthesis and remodeling were affected with a strong induction of genes coding for oxidative cross-linking enzymes, putatively associated with lignin related oxidative processes, including two laccases (L2E82_21065, $log_2FC = 8.4$; L2E82_21068, $log_2FC = 7.7$), two peroxidases (cationic peroxidase 1, L2E82_01414, $log_2FC = 8.8$; peroxidase 4, L2E82_00550, $log_2FC = 7.4$), a callose synthase 9 (L2E82_19626, $log_2FC = 7.1$) and five CASP-like proteins (CASP-like 1: L2E82_48627, $log_2FC = 7.3$; L2E82_48625, $log_2FC = 6.0$; CASP-like 5A2: L2E82_32609, $log_2FC = 1.3$; CASP-like 5B3: L2E82_32244, $log_2FC = 1.2$; CASP-like 5B2: L2E82_12781, $log_2FC = 1.0$). It is worth noting also the up-regulation of a transcript annotated as basic blue protein (L2E82_27998, $log_2FC = 6.6$) and its close relative annotated as uclacyanin 1 (L2E82_10797, $log_2FC = 8.3$), belonging to the phytocyanin family of extracellular type-I blue-copper proteins and related to lignin pathway (Zhu et al. 2018; Reyt et al. 2020). A gene coding for an expansin (L2E82_32200, $log_2FC = 1.94$) was also found to be slightly up-regulated, together with a gene encoding a cellulose synthase-like protein E1 (L2E82_46075, $log_2FC = 3.73$).

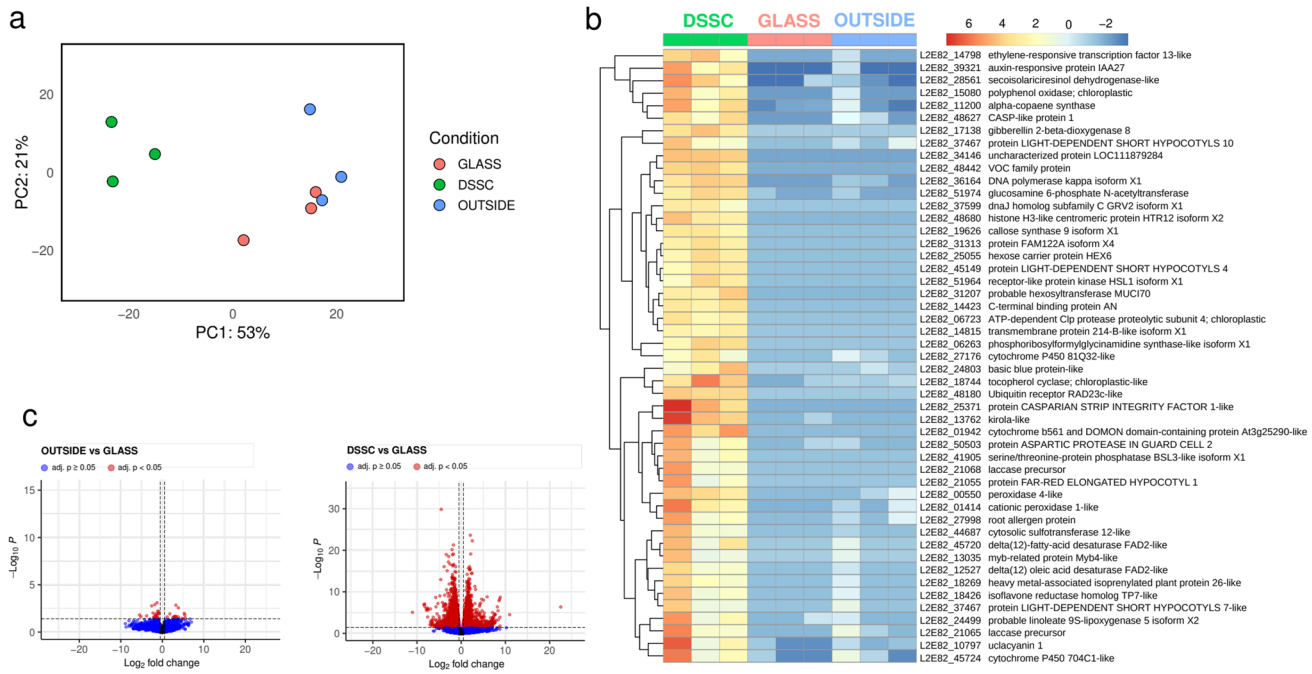


Fig. 2 Transcriptomic profiles of the radicchio plants. In (**a**), PCA on normalized read counts to visualize the differences in transcriptomic patterns across samples; in (**b**), heatmap depicting the 50 genes most variable in terms of expression between DSSC, OUTSIDE and GLASS samples, with hierarchical clustering of DEGs using the McQuitty algorithm and different colour intensity indicates different levels of expression based on normalized values of the transcript counts; in (**c**), volcano plots showing the differentially expressed genes (adjusted $p < 0.05$; red dots) in OUTSIDE (70) and DSSC (4,161) samples compared to controls (GLASS)

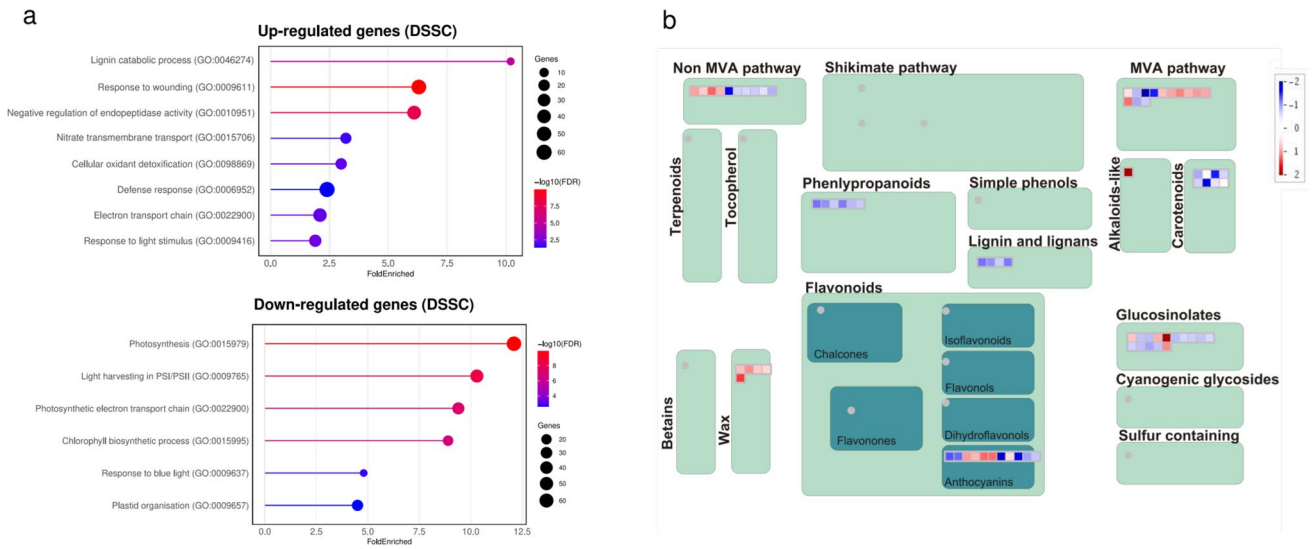


Fig. 3 Functional enrichment and metabolic mapping of DSSC RNA-seq data. In (**a**), GO terms related to biological process significantly enriched among up- and down-regulated genes in DSSC samples; in (**b**), MapMan view of secondary metabolic pathways showing the activation of cuticular-wax biosynthesis and repression of photosynthetic, carotenoid and lignin/lignan biosynthetic pathways

Additionally, genes involved in xyloglucan remodeling were also differentially expressed under DSSC. In particular, a gene coding for a xyloglucan endotransglucosylase/hydrolase was up-regulated (L2E82_12231; $\log_2FC = 2.85$), together with a gene encoding a xyloglucan-specific galacturonosyltransferase 1 (L2E82_06319; $\log_2FC = 1.47$). On the other hand, ten genes coding for cellulose synthase-related proteins, i.e. seven putative cellulose synthase A (CESA; L2E82_20178, L2E82_21291, L2E82_39509, L2E82_39904, L2E82_27934, L2E82_49311, L2E82_49303; $\log_2FC$ = -2.63, -1.12, -1.09, -0.74, -1.40, -0.73, and −0.67, respectively) and three CELLULOSE

SYNTHASE INTERACTIVE proteins (CSI; L2E82_34392, L2E82_18092, L2E82_17919; log_2FC = -1.39, -1.15, and −1.14, respectively), were down-regulated in DSSC samples compared to GLASS ones. Additionall In addition to genes involved in cell wall metabolism, transcriptomic data showed that transport was also affected by the presence of DSSC, as reflected by the up-regulation of genes coding for a glucose carrier HEX6 (L2E82_25055, $log_2FC = 7.1$), a chloroplastic Na^+/pyruvate antiporter BASS2 (L2E82_14296, $log_2FC = 5.2$), two aquaporins (TIP1-1, L2E82_31411, $log_2FC = 5.9$; PIP1-2, L2E82_40774, $log_2FC = 5.5$), and an ABC-G transporter (L2E82_51959, $log_2FC = 5.3$). Several members of the NRT1/PTR family were up-regulated (L2E82_24650, L2E82_06206, L2E82_27282, L2E82_46908, L2E82_07395; $log_2FC = 2.55$, 2.52, 2.36, 1.17, 0.88, respectively) (Table S3). Some genes putatively related to biosynthesis and catabolism of specialized metabolites were also up-regulated in DSSC samples compared to GLASS. Among them, genes coding for two cytochrome P450 monooxygenases, CYP704C1 (L2E82_45724, $log_2FC = 7.5$) and CYP81Q32 (L2E82_27176, $log_2FC = 6.3$), a germacrene A synthase (L2E82_11200, $log_2FC = 6.3$) and a β-amyrin 28-oxidase (L2E82_10518, $log_2FC = 6.3$). Among the down-regulated DEGs in the same condition, genes related to the xanthophyll pathway were identified, including *CRTISO* encoding a carotenoid isomerase (L2E82_20428, log_2FC = -0.8), *LCYB* encoding a lycopene β-cyclase (L2E82_01059, log_2FC = -0.9), and a zeaxanthin epoxidase (L2E82_43989, log_2FC = -1.10). Two genes coding for the flavonol kaempferol 3-O-beta-D-galactosyltransferases (L2E82_12213, log_2FC= -2.12; L2E82_12214, log_2FC = -2.42) were also found to be down-regulated. Light and hormone signalling modules were also activated, and genes coding for shade- and hormone-responsive regulators were found to be strongly up-regulated. The main effect of the DSSC cover modules on the radicchio shoot transcriptome was in fact mirrored by the modulation of the expression of specific light-responsive genes. In the DEG dataset of DSSC samples, fifteen key genes related to the response to light stimulus were identified (Table 1). Two genes coding for putative LIGHT-DEPENDENT SHORT HYPOCOTYLS paralogues (LSH10, L2E82_37467, $log_2FC = 6.66$; LSH4, L2E82_45149, $log_2FC = 2.95$) were among the up-regulated ones. In Arabidopsis, these proteins, namely ALOG/LSH proteins, act downstream of far-red (FR) and low-blue cues to promote cell expansion in cotyledons and stems (Vo Phan et al.2023). Particularly, LSH3/4 promote hypocotyl and cotyledon cell expansion under far-red-enriched or blue-depleted light (Roig-Villanova and Martinez-Garcia 2024; Takeda et al. 2024) and LSH10 is transcriptionally activated by neighbour shade signals (Vo Phan et al. 2023). Their induction in our dataset was observed together with the up-regulation of two genes involved in GA synthesis, coding for a gibberellin 20-oxidase (L2E82_22067, $log_2FC = 1.17$) and a gibberellin 2-beta-dioxygenase (L2E82_17138, $log_2FC = 5.66$), and with the transcription factor PIF3 (L2E82_01528, $log_2FC = 1.81$) known to play an essential role during shade-avoidance response (Han et al. 2024) (Table 1).

Notably, the orthologue of the Arabidopsis histone de-ubiquitinase OTLD1 (Vo Phan et al. 2023; L2E82_20298 in the radicchio dataset) was significantly down-regulated under DSSC filtered light (log_2FC = -1.33; Table S4) compared to GLASS, suggesting that chromatin de-ubiquitination may be reduced in this condition. Additionally, the down-regulation of genes coding for a protein WEAK CHLOROPLAST MOVEMENT UNDER BLUE LIGHT 1 (L2E82_17494, log_2FC = -1.13) and a blue-light photoreceptor PHR2 (L2E82_19828, log_2FC = -1.26) suggests that the plant reduced need for blue-light under the DSSC cover. It is also worth noting that two genes involved in the chlorophyll biosynthetic pathways were found to be down-regulated, i.e., a gene coding for a chlorophyllide an oxygenase (L2E82_26610, log_2FC = -0.69) and a chlorophyll a-b binding protein 7 (L2E82_36523, log_2FC = -0.89) (Table 1). Genes coding for other transcription factors (TFs) or proteins involved in hormonal signaling pathways also resulted to be up-regulated. Among them, it is worth noting an ethylene-responsive factor (L2E82_14798, $log_2FC = 6.9$), a MYB TF (MYB14; L2E82_13035, $log_2FC = 6.6$), a brassinosteroid-responsive RING protein 1 (BRH1; L2E82_13929, $log_2FC = 5.63$), and a brassinosteroid-targeted phosphatase BSL3 (L2E82_41905, $log_2FC = 7.3$), a linoleate 9-lipoxygenase (L2E82_24499, $log_2FC = 6.4$) and a Δ^{12}-desaturase DES8.11 (L2E82_45720, $log_2FC = 6.7$). Moreover, two auxin-responsive genes, i.e., *iaa27* (L2E82_39321, log2FC = 3.13) and an auxin-induced *PCNT115* homologue (L2E82_34913, log2FC = 2.06), were also up-regulated (Table S3).

Mercaptor4/Mapman annotation showed that WAX biosynthetic pathways were activated, while other pathways, such as lignin/lignan, phenylpropanoid and carotenoid biosynthesis seemed repressed (Fig. 3b), consistent with plant responses to a shaded environment. Activation of wax biosynthesis was supported by the induction of some key enzymatic steps, including genes coding for a 3-ketoacyl-CoA synthase 1 (L2E82_00220, $log_2FC = 2.54$; Todd et al. 1999) and a wax-ester synthase/diacylglycerol acyl-transferase 11-like (L2E82_51275, $log_2FC = 3.61$), together with the genes coding for their upstream regulators, such as the MIXTA-like transcription factor MYB16 (L2E82_33454, $log_2FC = 0.91$; Oshima and Mitsuda 2013) and the fatty-acid exporter FAX1 (L2E82_01020, $log_2FC = 0.67$), whose overexpression in Arabidopsis has been shown to boost both

Table 1 List of DEGs related to response to light stimulus in DSSC samples

Gene_ID	NCBI accession number	Log2FoldChange	Description	Best blastp hit on A. thaliana refseq_protein database (NCBI accession number)	% identity	Query coverage	e-value
L2E82_37467	KAI3708300.1	6.66	protein LIGHT-DEPENDENT SHORT HYPOCOTYLS 10 (LSH10)	LIGHT-DEPENDENT SHORT HYPOCOTYLS-like protein (DUF640) (NP_565978.1)	75.78%	79%	1e-82
L2E82_17138	KAI3767057.1	5.66	gibberellin 2-beta-dioxygenase 8	2-oxoglutarate (2OG) and Fe(II)-dependent oxygenase superfamily protein (NP_200674.1)	41.38%	38%	2e-06
L2E82_45149	KAI3700518.1	2.95	protein LIGHT-DEPENDENT SHORT HYPOCOTYLS 4 (LSH4)	LIGHT-DEPENDENT SHORT HYPOCOTYLS-like protein (DUF640) (NP_565716.1)	74.05%	87%	4e-87
L2E82_50011	KAI3682237.1	1.40	light-regulated protein 1, chloroplastic	CCR-like protein (NP_189308.1)	52.14%	88%	2e-03
L2E82_22067	KAI3751051.1	1.17	gibberellin 20 oxidase 1-B	gibberellin 20 oxidase 2 (NP_199994.1)	64.19%	77%	6e-180
L2E82_21055	KAI3750420.1	1.05	protein FAR-RED ELONGATED HYPOCOTYL 1	far-red elongated hypocotyl 1 (NP_001078018.1)	65.96%	22%	2e-10
L2E82_39677	KAI3709909.1	-0.79	phytochrome E	phytochrome E (NP_193547.4)	60.63%	97%	0.0
L2E82_36523	KAI3724735.1	-0.89	chlorophyll a-b binding protein 7, chloroplastic	Chlorophyll A-B binding family protein (NP_177783.1)	78.60%	89%	7e-173
L2E82_27913	KAI3737898.1	-0.93	phytochrome B	phytochrome B (NP_179469.1)	77.50%	98%	0.0
L2E82_02663	KAI3789859.1	-1.01	protein PHYTOCHROME-DEPENDENT LATE-FLOWERING	nuclear receptor coactivator (NP_001321648.1)	45.25%	100%	0.0
L2E82_26610	KAI3736665.1	-0.69	chlorophyllide a oxygenase, chloroplastic	Pheophorbide a oxygenase family protein with Rieske 2Fe-2 S domain-containing protein (NP_175088.1)	75.85%	100%	0.0
L2E82_30485	KAI3740067.1	-0.66	protein MAINTENANCE OF PSII UNDER HIGH LIGHT 1	proline-rich family protein (NP_568178.1)	57.42%	75%	5e-72
L2E82_11190	KAI3781185.1	-0.84	light-inducible protein CPRF2	bZIP transcription factor family protein (NP_568508.2)	41.71%	98%	9e-76
L2E82_17494	KAI3767395.1	-1.13	protein WEAK CHLOROPLAST MOVEMENT UNDER BLUE LIGHT 1	WEAK CHLOROPLAST MOVEMENT UNDER BLUE LIGHT-like protein (NP_001325286.1)	52.68%	93%	0.0
L2E82_19828	KAI3749221.1	-1.26	blue-light photoreceptor PHR2 isoform X2	photolyase/blue-light receptor 2 (NP_182281.1)	61.97%	99%	3e-180

cuticular wax and seed-oil accumulation (Li et al. 2015) (Table S3).

In contrast to the extensive transcriptional remodelling seen under the applied DSSC, OUTSIDE condition did not strongly affect the radicchio transcriptome. Only 21 up-regulated and 49 down-regulated genes *versus* GLASS samples were identified. Among the up-regulated transcripts in OUTSIDE-grown radicchio plants (Table S4), some small functional clusters have been distinguished. Signalling components were activated, such as a gene coding for a receptor-like serine/threonine kinase (L2E82_40153, $log_2FC = 5.4$), a NAC transcription factor 56 (L2E82_46252, $log_2FC = 5.3$) and a Ca^{2+} sensor (CML41; L2E82_19072, $log_2FC = 3.3$). Some genes involved in membrane trafficking and redox control were also found to be up-regulated, including a clathrin-assembly protein (L2E82_47152, $log_2FC = 3.9$), a glycerophosphodiester phosphodiesterase (L2E82_26844, $log_2FC = 3.8$) and a glutathione S-transferase (L2E82_11703, $log_2FC = 3.6$). Conversely, the down-regulated genes were mainly associated with primary

metabolism components, such as genes related to sterol biosynthesis (δ-24-sterol reductase, L2E82_14119, log_2FC = -7.06) and central-carbon enzymes such as a pyrophosphate-dependent phosphofructokinase (L2E82_24979, log_2FC = -6.38) and a fumarate hydratase (L2E82_15525, log_2FC = -5.61), which were identified as strongly repressed compared to the GLASS condition (Table S4).

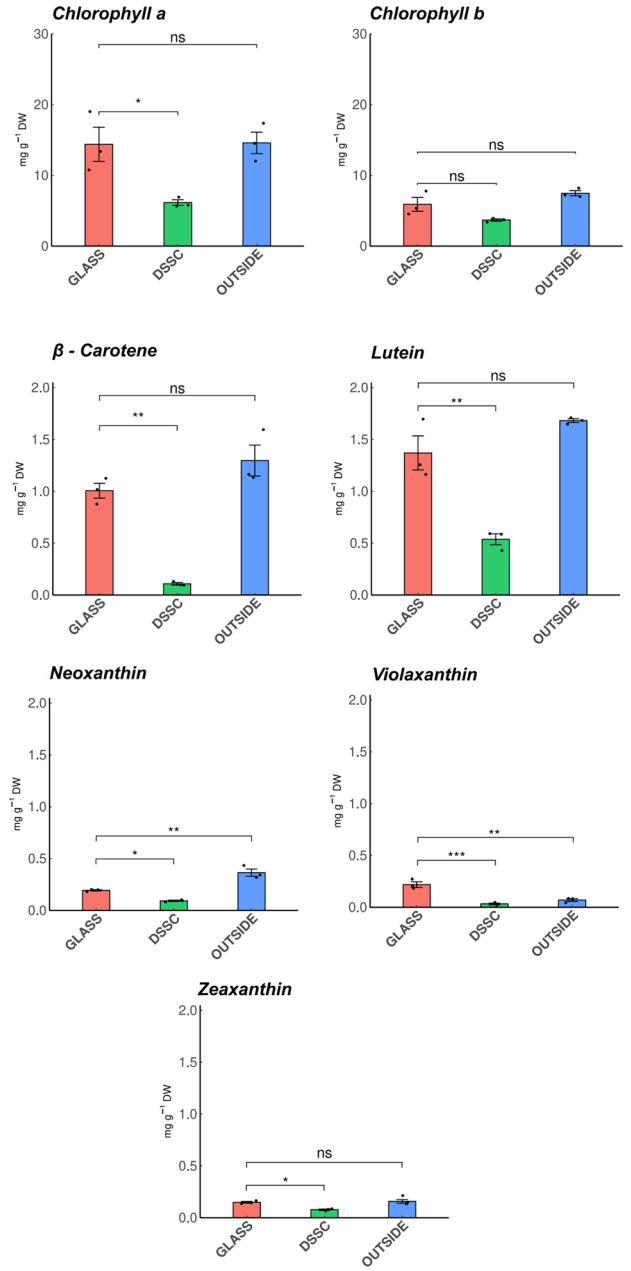


Fig. 4 Carotenoid content in radicchio plants. Contents (mg g^{-1} DW) of carotenoids (neoxanthin, violaxanthin, zeaxanthin, lutein, β-carotene) and chlorophylls (Chl a, Chl b) in shoots of plants grown under customized-DSSC, GLASS and OUTSIDE. Bars show mean ± SE (n = 3). Asterisks indicate significant differences from the GLASS control (ANOVA + Tukey, $p \leq 0.05$; ns, *, **, ***: not significant or significant at $p \leq 0.05$, $p \leq 0.01$, and $p \leq 0.001$, respectively)

Photosynthetic Pigments and Polyphenols Content

The main photosynthetic pigments detected in *C. intybus* leaves were neoxanthin, violaxanthin, lutein, zeaxanthin, chlorophyll b, chlorophyll a, and β-carotene (Figure S3). One-way ANOVA showed that light filtered through the dye-sensitized solar cell (DSSC) panels affected all carotenoid contents (Fig. 4 and Table S5). Particularly, neoxanthin (One-way ANOVA F-value = 15.35, p-value = 0.0031), violaxanthin (F = 14.11, p-value = 0.0038), and zeaxanthin (F = 5.93, p-value = 0.0337) contents were all significantly lower in DSSC samples than in GLASS-covered controls. DSSC plants accumulated between 1.5- and 2-fold fewer neoxanthin and violaxanthin, respectively, and approximately 40% less lutein (F = 4.85, p-value = 0.0005) and β -carotene (F = 9.68, p-value = 0.0132) than the control (GLASS) condition. In addition, while chlorophyll b content did not differ between GLASS and DSSC samples, chlorophyll a was significantly lower in plants under DSSC than in control, representing roughly a 25% depletion and reducing the chlorophyll a/b ratio only under DSSC light. In contrast, exposure to sunlight without any cover (OUTSIDE samples) produced only minor adjustments compared to control. β-carotene, lutein, zeaxanthin, and chlorophyll a and b contents did not differ between OUTSIDE and GLASS samples. A slight but significant increase in neoxanthin and a modest decrease in violaxanthin were observed, but no broader pattern emerged. The lack of difference in carotenoid content between the OUTSIDE and GLASS samples was probably related to the high variability within the limited number of replicates (n = 3). Concerning DSSC samples, on the other hand, the data show that DSSC-filtered spectra selectively inactivate the xanthophyll-related pathway.

Regarding phenylpropanoids, in the three main classes of compounds detected in the extracts, caffeic acid derivatives, flavonols and epigallocatechin derivatives (Figure S4), different accumulation was observed across the three conditions (Fig. 5 and Table S6). Caffeic acid derivatives were affected by the condition (one-way ANOVA F-value = 18.27, p-value = 0.0028), and they were induced in OUTSIDE samples, reaching nearly 1 mg g^{-1} DW, while no significant differences were detected between GLASS and DSSC samples. A similar outcome was obtained with the data on the concentration of epigallocatechin derivatives (F = 9.29, p-value = 0.0146), which, overall, showed a higher level of accumulation compared to caffeic acid derivatives and flavonoids. These compounds were significantly higher in OUTSIDE samples, while again no differences were identified between GLASS and DSSC plants. The only detected flavonoid, at very low concentration, was represented by kaempferol-3-O-glucuronide, and it was affected by the

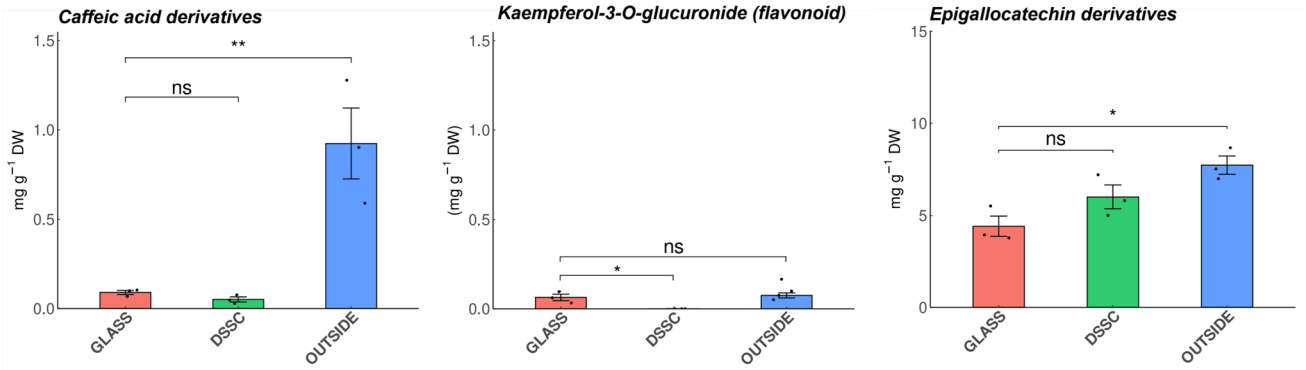


Fig. 5 Phenylpropanoid content in radicchio plants. Contents (mg g^{-1} DW) of polyphenols (caffeic acid and epigallocatechin derivatives, kaempferol-3-O-glucuronide) in shoots of plants grown under customized-DSSC, GLASS and OUTSIDE. Bars show mean ± SE ($n = 3$). Asterisks indicate significant differences from the GLASS control (ANOVA + Tukey, $p \leq 0.05$; ns, *, **, ***: not significant or significant at $p \leq 0.05$, $p \leq 0.01$, and $p \leq 0.001$, respectively)

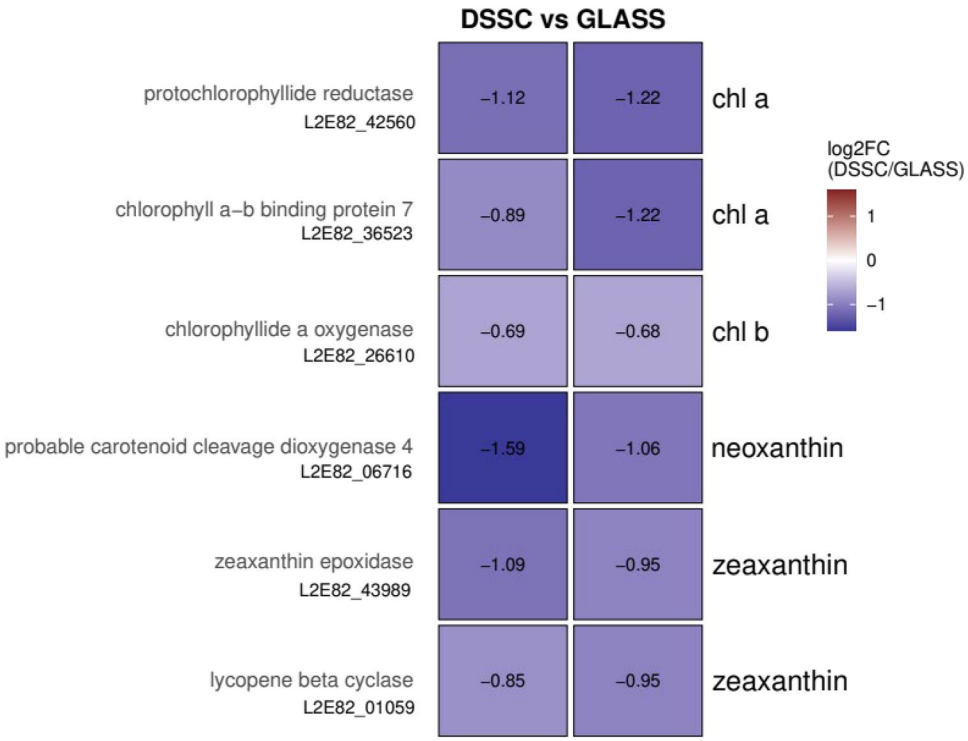


Fig. 6 Gene–carotenoid paired panels (DSSC vs. GLASS). For each pair, the left square reports the gene log_2FC (DSSC vs. GLASS) and the right square the matched pigment log_2FC (DSSC vs. GLASS). Values are shown inside tiles; color encodes effect size (blue = down in DSSC, red = up in DSSC)

condition factor (F = 8.52, p-value = 0.0176). Compared to the other analysed phenylpropanoids, kaempferol-3-O-glucuronide showed an opposite trend. It was detectable in GLASS and OUTSIDE samples, while absent in DSSC plants. Both GLASS and OUTSIDE samples showed modest accumulation (approximately 0.06–0.08 mg g^{-1} DW).

Using within-feature standardization, the pooled Pearson correlation on z-scores was significant ($r = 0.80$, p-value = 4.8×10^{-9}), suggesting that variation in gene expression correlates with the corresponding pigment levels across conditions (Fig. 6).

Discussion

The interest in semi-transparent PV panels for agrivoltaic applications is exponentially increasing. By providing partial shade, PV modules may reduce evaporation rates, helping to preserve soil moisture and improve water-use efficiency (Semeraro et al. 2024; Hickey et al. 2024). Since their introduction in the early 1990s, DSSCs have shown promising results in terms of the trade-off between electrical yield and absorbed/transmitted radiation, mainly due to their tuneable colour and semitransparency, features that make them appealing for photovoltaics (Barichello et al. 2024). However, studies on how DSSC-filtered light can

affect plant growth, secondary metabolites, and molecular responses are still scarce. In this work, a far-red-enriched, blue-depleted light spectrum, together with a reduced light intensity (lower PPFD) transmitted through a customized-DSSC panel, impacted the radicchio phenotype, the whole transcriptomic profile, as well as carotenoid and flavonol contents.

Growth of the Plants under the Customized-DSSC Cover Panel Led to Phenotypes that were Mirrored by the Modulation of Cell Wall Related Transcripts

The presence of a customized-DSSC with BTD-DTP1 dye and TiO_2 embedded did not affect *C. intybus* seed germination, in agreement with what has been recently reported for the same radicchio genotype under a semi-transparent perovskite layer (Spampinato et al. 2025). However, plants grown under the customized-DSSC, compared to those grown under a glass panel or without cover, showed a distinct phenotype mainly related to shade avoidance syndrome (SAS; Li and Wang 2022). Specifically, the used DSSC panel induced reduced leaf expansion and increased hypocotyl elongation during the early seedling stage, symptoms previously well described in plants affected by SAS (Martínez-García et al. 2010; Li and Wang 2022).

It is worth noting that the phenotype of plants grown under the customized-DSSC, showing elongated stems, can be linked to the induction of an expansin-A6. Expansins, in fact, are key regulators of cell wall elongation during plant growth, being involved in the loosening and extension of plant cell walls by disrupting non-covalent bonding between cellulose microfibrils and matrix glucans (Shcherban et al. 1995; Cosgrove 2024a). The DSSC-filtered light also induced the up-regulation of genes coding for two laccases, two peroxidases and five CASP-like proteins, all of which play a role in secondary plant cell wall modification (Roppolo et al. 2011; Zhao et al. 2013). In this context, it is also worth noting the induction of the genes coding for a phytocyanin basic-blue-protein and a uclacyanin 1, considering the reported role of blue copper proteins in lignin domain formation in the Casparian strip (Reyt et al. 2020). Thus, DSSC-filtered light appears to trigger the activation of a putative expansin gene involved in loosening the primary cell wall and in allowing petiole elongation (Cosgrove 2024b), as well as the regulation of genes related to primary and secondary cell wall composition, probably for preserving cell structural integrity despite the fast growth. In particular, it is worth noting that some genes involved in xyloglucan remodeling and a gene coding for a cellulose synthase-like protein were induced in DSSC samples, while several CESA/CSI genes were found to be down-regulated (mean log_2FC for CESA = -1.21), suggesting a shift toward matrix polysaccharide remodeling and confirming the link between cell wall remodeling and shade avoidance response (Tang and Liesche 2017). Our results agree with the connection between shade avoidance response and cell wall remodeling reported in Arabidopsis and tomato (Tang and Liesche 2017; Cagnola et al. 2012), although the direct effect on cell wall composition must still be investigated using specific cell wall probes (e.g., monoclonal antibodies) for microscopic observations. Notably, a simultaneous induction of some receptor-like kinases and transcription factors in plants grown without cover may suggest a fine-tuning of gene expression rather than a broader acclimation process. Up-regulation of clathrin-assembly and lipid-recycling enzymes, together with a glutathione S-transferase, may imply small adjustments in membrane turnover and antioxidant capacity (Marrs 1996; Yu et al. 2021). It could also be hypothesised that direct irradiance from lamps to plants, without any cover, generates a demand for energy dissipation. In this scenario, in addition to the up-regulation of some genes related to antioxidant processes, the significant accumulation of neoxanthin in plants grown without cover compared to controls may suggest the need for this photoprotective pigment, which is directly involved in photoprotection as an antioxidant, besides its indirect role in chlorophyll-to-carotenoid triplet transfer (Dall'Osto et al. 2007).

Radicchio Plants Developed under the DSSC Activate Light and Hormone Related Pathways Linked to Shade Avoidance Response

Consistent with their phenotype, transcriptomic profiles of plants grown under the customized-DSSC revealed the activation of metabolic changes correlated with the response to shade and SAS. Transcriptome-wide analyses in plants have shown that SAS is driven by a phytochrome-interacting-factor (PIF) hub, which up-regulates hormonal pathways, cell wall-loosening and lipid-remodelling genes while repressing photosynthesis, reallocating resources toward elongation (Casal and Fankhauser 2024). Under the used DSSC panel, it seems that plants reallocate carbon and energy from photoprotection to rapid elongation, a classic growth-stress response trade-off. Two ALOG regulators were induced, i.e., *LSH10* and its paralogue *LSH4*. Arabidopsis studies have demonstrated the interaction between the ALOG transcription factor LSH10 and the histone-deubiquitinase OTLD1 to create a complex involved in balancing growth and defence under shade conditions (Vo Phan et al. 2023). Additionally, several transcripts identified as typical markers of the SAS are significantly up-regulated in the plants grown under DSSC. The up-regulation of the gene coding for FAR-RED ELONGATED HYPOCOTYL 1

(FHY1), known to be required for R: FR spectrum-specific plant responses and crucial for plant adaptation to changing light conditions (Chen et al. 2012), is one remarkable example. This result suggests that the plant perceives a light quality shift toward FR, with low R: FR ratio, consistent with conditions such as the growth under DSSC modules or canopy shade. Similarly, the induction of a gene coding for the transcription factor PIF3, one of the master regulators of the bHLH shade-avoidance cascade, indicates shade avoidance response, since PIF3 integrates phytochrome signals and promotes elongation under low R: FR light conditions (Toledo-Ortiz et al. 2014; Han et al. 2024). The down-regulation of the two genes coding for phytochrome B and E is another footprint of the shade avoidance response of plants grown under DSSC modules. The disruption of phyB in *Arabidopsis* results in constitutive shade avoidance responses, indicating that phyB is a key negative regulator of these responses (Reed et al. 1993). In tomato, it has been demonstrated that the phyB paralogue, phyE, may act redundantly with phyB in modulating SAS (Schrager-Lavelle et al. 2016). Thus, the down-regulation of both phyE and phyB homologues in radicchio plants grown under DSSC suggests the inactivation of these two phytochromes, leading to a shade avoidance response. Additionally, the down-regulation of genes coding for a protein WEAK CHLOROPLAST MOVEMENT UNDER BLUE LIGHT 1 and a blue-light photoreceptor PHR2 can be linked to the reduced light intensity and altered light spectrum, and subsequently light quality, filtered by the DSSC. Both genes are indeed part of the plant blue-light response machinery: the first has been reported to help the movement of chloroplasts triggered by intense blue light (Kodama et al. 2011), and PHR2 is a photolyase-type protein that repairs UV/blue-induced DNA damage (Kanai et al. 1997). Hence, it could be argued that the low-blue/UV environment created by the customized-DSSC panel also affected the expression of the blue/UV light-related pathways, that were down-regulated since blue light is depleted/reduced. The shade effect could also be linked to the enhanced nitrate transport indicated by transcriptomic data. The up-regulation of several NRT1/ PTR transporters in plants grown under customized-DSSC compared to both controls and plants without cover suggests that nitrate is translocated and likely accumulated in the shoots. Notably, in lettuce and rocket grown under opaque PV panels, a nitrate accumulation in the leaves has been reported, consistently linked with a shading effect (Khan et al. 2018; Hickey et al. 2024). Lastly, it is known from the literature that the PAR transmittance of the DSSC panel can be approximately 40% (Selvaraj et al. 2019), which means that the effective PPFD perceived by the plants under the panel could be lower than the incident PPFD. In fact, PAR transmittance for the DSSC panel with semi-transparent DSSC devices for building/greenhouse applications has been estimated as 37–53% (Selvaraj et al. 2019). Studies on different BTD-DTP dyes show visible transmittance in the range of approximately 17–48%, depending on the dye loading and TiO_2 thickness (Dessì et al. 2021). Thus, considering the spectral filtering properties of DSSCs, the typical SAS phenotype and the associated transcriptomic remodelling could be due to the changes in both spectral quality and reduction in light intensity.

Hormone metabolism and signalling also showed a shift in DSSC samples when compared to plants grown under glass or without cover. Particularly, the genes coding for a GA 2-beta-dioxygenase and a GA 20 oxidase, as well as the brassinosteroid-related protein BSL3 phosphatase and the brassinosteroid-responsive RING protein 1 (BRH1), were strongly up-regulated. Shade has been documented to boost brassinosteroid (BR) signalling: BR biosynthesis mutants (*dwarf1* and *rot3*) fail to elongate under shading conditions, and bioactive BR levels rise in simulated shade (Luccioni et al. 2002; Bou-Torrent et al. 2014; Huang et al. 2022). At the same time, shading is known to affect the expression of gibberellin (GA) biosynthetic genes, including the two detected in DSSC DEG dataset, and, after longer exposure, the GA content itself in plants (Hisamatsu et al. 2005; Bou-Torrent et al. 2014; Liu et al. 2021). Additionally, the up-regulation of auxin- and ethylene-responsive genes further supports the idea that the customized-DSSC filtered light engages the hormonal pathways associated with the shade avoidance growth (Vandenbussche et al. 2003, 2005). Hypocotyl elongation in shade avoidance requires auxin (Du et al. 2018). Moreover, low R: FR light is known to inactivate phytochrome B and promote ethylene production within minutes to hours of shade exposure (Pierik et al. 2004). Nevertheless, further analyses focused on characterisation and quantification of hormones in shoots of plants developed under DSSC panels will be pivotal to verify their physiological response during growth under the panels.

A Decrease in Carotenoid Content in Plants Grown under DSSC Modules Suggests Low Photoprotection Demands

Although seedling elongation is the best-characterised outcome of the SAS, a low R: FR ratio is known to lead to a decrease in the accumulation of photosynthetic pigments, including carotenoids (Bou-Torrent et al. 2015; Sng et al. 2020). Not surprisingly, a significant decrease in carotenoid content, including lutein, β-carotene, neoxanthin, violaxanthin, and zeaxanthin, was observed in radicchio plants grown under DSSCs. Transcriptome data on carotenoid-related genes partially reflect the biochemical results. The Pearson correlation on z-scores of selected genes related to pigment

pathways was significant, indicating that the expression of these genes was presumably linked to the corresponding pigment levels across conditions. This result may support a coordinated adjustment of the carotenoid/chlorophyll pathways under the DSSC light regime. Genes related to the xanthophyll pathway, such as those coding for a carotenoid isomerase and a lycopene β-cyclase, were found to be down-regulated compared to control plants grown under the glass panel. The down-regulation of a gene coding for a zeaxanthin epoxidase may also be directly linked to the strong decrease in this carotenoid in plants grown under DSSC. In plants, the conversion of zeaxanthin to violaxanthin in the xanthophyll cycle is crucial for an efficient dissipation of the excess excitation energy (Bugos et al. 1999). Violaxanthin de-epoxidase is located in the thylakoid lumen, while zeaxanthin epoxidase is positioned on the stromal side, on the opposite faces of the membrane (Havaux and Niyogi 1999; Hieber et al. 2000). It has been documented that, under low light levels, zeaxanthin is converted to its epoxidated form violaxanthin for an efficient light absorption while under high light levels zeaxanthin promotes LHCII aggregation, a state in which this antenna complex is highly quenched (Bugos et al. 1999; Johnson and Ruban 2009). However, some studies in controlled conditions have reported that FR light or low R: FR ratios might decrease the accumulation of all carotenoids, including xanthophylls, in lettuce (Li and Kubota 2009; Van Brenk et al. 2024). Accordingly, a simultaneous decline in zeaxanthin and, even more significant, in violaxanthin may indicate that DSSC-filtered light affects the entire xanthophyll cycle in radicchio plants rather than merely regulating the epoxidation of zeaxanthin. It could be argued that, beneath the customized-DSSC panel, plants did not sense a significant reduction in photosynthetic photon-flux density (PPFD), which refers to light quantity, and the xanthophyll cycle, normally modulated by light intensity (Demmig-Adams and Adams 1996), is depleted.

The chlorophyll content findings also align with the RNA-seq data. In DSSC samples, the "chlorophyll biosynthetic process" GO term is significantly over-represented among down-regulated genes, together with broader photosynthetic categories such as "Photosynthesis" and "Light harvesting in PSI/PSII". The dataset of down-regulated genes includes, for example, a chlorophyllide a oxygenase (CAO) and a chlorophyll a/b-binding protein. Particularly, CAO is the enzyme that converts chlorophyll a to chlorophyll b after an oxygenation reaction (Dey et al. 2023). Thus, the significantly reduced content of chlorophyll a in DSSC samples, together with the unaffected chlorophyll b accumulation and the down-regulation of the CAO-encoding gene, can be associated with a shade-acclimation profile, achieved mainly by reducing chlorophyll a synthesis.

Taken together, the observed low xanthophyll content in plants grown under the customized-DSSC appears to be associated with the reduction of their photosynthetic activity, with a consequent reduced demand for non-photochemical quenching. In brief, DSSC panels create a spectral environment associated with shading that affects carotenoid induction, imposes FR-triggered repression, and decreases the need for photoprotective pigments, explaining the decrease in neoxanthin, violaxanthin, β-carotene and lutein observed in these plants.

Regarding polyphenols, the plants grown under the glass panel and those grown under the customized-DSSC showed similar concentrations of caffeic acid and epigallocatechin derivatives, suggesting that the customized-DSSC panel did not affect the accumulation of these compounds. The lack of differences in caffeic acid and epigallocatechin derivatives between DSSC and GLASS likely reflects similar spectral filtering: the DSSC panel reduces UV/blue wavelengths that stimulate phenolic biosynthesis, and the used glass also attenuates much of the same range, yielding comparable outcomes. On the other hand, the flavonol kaempferol-3-O-glucuronide was completely absent in plants grown under the customized-DSSC. This qualitative change aligns with the RNA-seq data, which showed the down-regulation of two paralogous kaempferol 3-O-β-D-galactosyltransferase genes in DSSC plants. In radicchio, it has been recently reported that kaempferol 3-O-glucuronide was the most represented compound in plants developed under red LEDs (Menicucci et al. 2025). Thus, it could be argued that the low R: FR ratio resulting from the use of the customized-DSSC panel attenuates the spectral range that favours kaempferol 3-O-glucuronide accumulation.

The Customized-DSSC Panel Can be Used to Modulate Plant Development

The use of the customized-DSSC panel can be of interest for shade-tolerant crops and for manipulating flowering time in controlled conditions. In response to a low R: FR ratio typical of shading and under canopy conditions, indeed, extension growth and flowering are enhanced in shade-avoiding species, while shade-tolerant species can delay flowering (Runkle and Heins 2001). Specifically, for several long-day plants, e.g., some ornamentals and lentils, adding FR to the photoperiod often speeds up flowering (Mobini et al. 2016), so the low R: FR under DSSC can shorten production cycles when early flowering is needed. By contrast, for several short-day plants (e.g., some basil cultivars; Stallknecht et al. 2023), a FR-rich environment may favour delayed flowering, which can be exploited to prolong the vegetative phase of leafy crops or delay harvest dates. For such species, the reduction in total photosynthetically active radiation (PAR)

might not be an issue, and the extra FR may even result in increased leaf area without compromising leaf thickness, as reported in basil and petunia (Stallknecht et al. 2023; Xia and Mattson 2024). Alternatively, the DSSC modules can be paired with dimmable LEDs that could supply the missing red/blue photons only when needed (e.g., specific plant life cycle phases; Stamford et al. 2023). The use of dimmable blue and red LEDs has been proven to be feasible for growing radicchio plants (*C. intybus* cv. Precoce and Tardiva), also as a tool for improving their nutraceutical (e.g., antioxidant polyphenols) content (Menicucci et al. 2025). Hence, DSSC panels might offer a passive way to accelerate or delay flowering by selecting species/genotypes with the appropriate day-length response, while their energy output can power corrective dimmable LEDs to prevent the shade avoidance syndrome (SAS) observed under passive shading.

Conclusions

In conclusion, this study provides the first transcriptomic and carotenoid/phenolic content profiles of *Cichorium intybus* plants cultivated beneath a semi-transparent customized-DSSC panel with BTD-DTP1 dye, under specific controlled conditions. Key results showed that the altered light environment, characterised by a low R: FR ratio with a reduced blue light and a reduced light intensity, induces a shade avoidance response and seems to favour the reallocation of carbon from photosynthetic and carotenoid pathways toward elongation, cell wall rearrangements and nitrate transport, simultaneously modulating hormone regulation typically associated with shade-avoidance responses.

Future research should focus on improving DSSC panel transparency through thinner TiO_2 layers and narrow/custom band dyes, to reduce shade responses while at the same time preserving electrical yield. It is worth noting that the advantage of using easy-to-prepare organic dyes compared to Ru-based ones allows for more straightforward modification of the molecular structure, in addition to lower costs and higher environmental benefits. This could enable fine-tuning of light absorption, which could be adapted to minimize undesired effects. Finally, the molecular (e.g., light-responsive genes, genes related to SAS) and biochemical (e.g., carotenoids) markers identified here might support the screening of plant species/genotypes tolerant to DSSC-filtered light spectra, as well as optimise DSSC materials and developing hybrid DSSC-LED lighting strategies aimed at minimising shade-avoidance while maximising agrivoltaic performance.

Supplementary Information The online version contains supplementary material available at https://doi.org/10.1007/s00344-026-12119-w.

Acknowledgements The work was supported by the CNR-funded project Vertigrow, CUP B15F21004410005.

Author Contributions Conceptualization: AD, GR, RB; Methodology: FS, AD, ES, GR, RB; Formal analysis and investigation: FS, AD, CB, FM, SB, ES; Writing - original draft preparation: FS, AD; Writing - review and editing: FS, AD, CB, FM, SB, GR, RB; Supervision: GR, RB. All authors read and approved the final manuscript.

Funding Open access funding provided by Consiglio Nazionale Delle Ricerche (CNR) within the CRUI-CARE Agreement.

Declarations

Conflict of interest The authors declare that they have no known competing financial interests or personal relationships that could have appeared to influence the work reported in this paper.

Ethical Approval This article does not contain any studies with human or animal subjects.

Open Access This article is licensed under a Creative Commons Attribution 4.0 International License, which permits use, sharing, adaptation, distribution and reproduction in any medium or format, as long as you give appropriate credit to the original author(s) and the source, provide a link to the Creative Commons licence, and indicate if changes were made. The images or other third party material in this article are included in the article's Creative Commons licence, unless indicated otherwise in a credit line to the material. If material is not included in the article's Creative Commons licence and your intended use is not permitted by statutory regulation or exceeds the permitted use, you will need to obtain permission directly from the copyright holder. To view a copy of this licence, visit http://creativecommons.org/licenses/by/4.0/.

References

Ashenafi EL, Nyman MC, Shelley JT, Mattson NS (2023) Spectral properties and stability of selected carotenoid and chlorophyll compounds in different solvent systems. Food Chem Adv 2:100178

Bais HP, Ravishankar GA (2001) *Cichorium intybus* L—cultivation, processing, utility, value addition and biotechnology, with an emphasis on current status and future prospects. J Sci Food Agric 81:467–484

Barichello J, Mariani P, Vesce L, Spadaro D, Citro I, Matteocci F, Bartolotta A, Di Carlo A, Calogero G (2024) Bifacial dye-sensitized solar cells for indoor and outdoor renewable energy-based applications. J Mater Chem C 12:2317–2349

Barron-Gafford GA, Pavao-Zuckerman MA, Minor RL, Sutter LF, Barnett-Moreno I, Blackett DT et al (2019) Agrivoltaics provide mutual benefits across the food–energy–water nexus in drylands. Nat Sustain 2:848–855

Bou-Torrent J, Galstyan A, Gallemí M, Cifuentes-Esquivel N, Molina-Contreras MJ, Salla-Martret M et al (2014) Plant proximity perception dynamically modulates hormone levels and sensitivity in *Arabidopsis*. J Exp Bot 65:2937–2947

Bou-Torrent J, Toledo-Ortiz G, Ortiz-Alcaide M, Cifuentes-Esquivel N, Halliday KJ, Martínez-García JF, Rodríguez-Concepción M (2015) Regulation of carotenoid biosynthesis by shade relies on

specific subsets of antagonistic transcription factors and cofactors. Plant Physiol 169:1584–1594
Bugos RC, Chang SH, Yamamoto HY (1999) Developmental expression of violaxanthin de-epoxidase in leaves of tobacco growing under high and low light. Plant Physiol 121:207–214
Cagnola JI, Ploschuk E, Benech-Arnold T, Finlayson SA, Casal JJ (2012) Stem transcriptome reveals mechanisms to reduce the energetic cost of shade-avoidance responses in tomato. Plant Physiol 160:1110–1119
Casal JJ, Fankhauser C (2024) Shade avoidance in the context of climate change. Plant Physiol 191:1475–1491
Chang S, Puryear J, Cairney J (1993) A simple and efficient method for isolating RNA from pine trees. Plant Mol Biol Rep 11:113–116
Chen F, Shi X, Chen L, Dai M, Zhou Z, Shen Y et al (2012) Phosphorylation of FAR-RED ELONGATED HYPOCOTYL1 is a key mechanism defining signaling dynamics of phytochrome A under red and far-red light in *Arabidopsis*. Plant Cell 24:1907–1920
Chowdhury FI, Blaine T, Gougam AB (2013) Optical transmission enhancement of fluorine doped tin oxide (FTO) on glass for thin film photovoltaic applications. Energy Procedia 42:660–669
Cosgrove DJ (2024a) Structure and growth of plant cell walls. Nat Rev Mol Cell Biol 25:340–358. https://doi.org/10.1038/s41580-023-00691-y
Cosgrove DJ (2024b) Plant cell wall loosening by expansins. Annu Rev Cell Dev Biol 40:329–352
Crippa M, Solazzo E, Guizzardi D, Monforti-Ferrario F, Tubiello FN, Leip A (2021) Food systems are responsible for a third of global anthropogenic GHG emissions. Nat Food 2:198–209
Dall'Osto L, Cazzaniga S, North H, Marion-Poll A, Bassi R (2007) The *Arabidopsis* aba4-1 mutant reveals a specific function for neoxanthin in protection against photo-oxidative stress. Plant Cell 19:1048–1064
Dayıoğlu MA, Turker U (2021) Digital transformation for a sustainable future—agriculture 4.0: a review. J Agric Sci 27:373–399
Demmig-Adams B, Adams WW III (1996) Xanthophyll cycle and light stress in nature: uniform response to excess direct sunlight among higher plant species. Planta 198:460–470
Dessì A, Calamante M, Sinicropi A, Parisi ML, Vesce L, Mariani P et al (2020) Thiazolo[5,4-d]thiazole-based organic sensitizers with improved spectral properties for greenhouse-integrated dye-sensitized solar cells. Sustain Energy Fuels 4:2309–2321
Dessì A, Chalkias DA, Bilancia S, Sinicropi A, Calamante M, Mordini A et al (2021) D–A–π–A organic dyes with tailored green-light absorption for potential application in greenhouse-integrated dye-sensitized solar cells. Sustain Energy Fuels 5:1171–1183
Dessì A, Spampinato C, Sillo F, Valastro S, Centritto M, Brunetti C, Ghirardo A, Schnitzler J-P, Alberti A, Reginato G, Rizzo A, Balestrini R (2025) Integrating tunable LED-induced plant responses with novel solar cell technologies for energy-efficient agrivoltaic systems. Plants People Planet Online Version. https://doi.org/10.1002/ppp3.70114
Dey D, Tanaka R, Ito H (2023) Structural characterization of the chlorophyllide a oxygenase (CAO) enzyme through an *in silico* approach. J Mol Evol 91:225–235
Dobin A, Davis CA, Schlesinger F, Drenkow J, Zaleski C, Jha S et al (2013) STAR: ultrafast universal RNA-seq aligner. Bioinformatics 29:15–21
Du J, Jiang H, Sun X, Li Y, Liu Y, Sun M et al (2018) Auxin and gibberellins are required for the receptor-like kinase ERECTA-regulated hypocotyl elongation in shade avoidance in *Arabidopsis*. Front Plant Sci 9:124
Fan W, Wang S, Wang H, Wang A, Jiang F, Liu H et al (2022) The genomes of chicory, endive, great burdock and yacon provide insights into Asteraceae palaeo-polyploidization history and plant inulin production. Mol Ecol Resour 22:3124–3140
Fernández-Milmanda GL, Ballaré CL (2021) Shade Avoidance: Expanding the Color and Hormone Palette. Trends Plant Sci 26:509–523
Hahn C, Lindkvist E, Magnusson D, Johansson M (2025) The role of agriculture in a sustainable energy system—the farmers' perspective. Renew Sustain Energy Rev 213:115437
Hainsch K, Löffler K, Burandt T, Auer H, Del Granado PC, Pisciella P, Zwickl-Bernhard S (2022) Energy transition scenarios: what policies, societal attitudes and technology developments will realize the EU. Green Deal? Energy 239:122067
Han R, Ma L, Terzaghi W, Guo Y, Li J (2024) Molecular mechanisms underlying coordinated responses of plants to shade and environmental stresses. Plant J 117:1893–1913
Havaux M, Niyogi KK (1999) The violaxanthin cycle protects plants from photo-oxidative damage by more than one mechanism. Proc Natl Acad Sci USA 96:8762–8767
Hickey T, Uchanski M, Bousselot J (2024) Vegetable crop growth under photovoltaic modules of varying transparencies. Heliyon 10:e36058
Hieber AD, Bugos RC, Yamamoto HY (2000) Plant lipocalins: violaxanthin de-epoxidase and zeaxanthin epoxidase. Biochim Biophys Acta Protein Struct Mol Enzymol 1482:84–91
Hisamatsu T, King RW, Helliwell CA, Koshioka M (2005) The involvement of gibberellin 20-oxidase genes in phytochrome-regulated petiole elongation of *Arabidopsis*. Plant Physiol 138:1106–1116
Huang S, Yang C, Li L (2022) Unravelling the dynamic integration of auxin, brassinosteroid and gibberellin in early shade-induced hypocotyl elongation. Phenomics 2:119–129
Johnson MP, Ruban AV (2009) Photoprotective energy dissipation in higher plants involves alteration of the excited-state energy of the emitting chlorophyll(s) in the light-harvesting antenna II. J Biol Chem 284:23592–23601
Kanai S, Kikuno R, Toh H, Ryo H, Todo T (1997) Molecular evolution of the photolyase–blue-light photoreceptor family. J Mol Evol 45:535–548
Khan KA, Yan Z, He D (2018) Impact of light intensity and nitrogen of nutrient solution on nitrate content in three lettuce cultivars prior to harvest. J Agric Sci 10:99–109
Kim J, Oh W (2024) Growth, flowering and morphological responses of petunia to light conditions in a greenhouse modified by dye-sensitized solar cells and LEDs. Hortic Environ Biotechnol 65:737–745
Kodama Y, Suetsugu N, Wada M (2011) Novel protein–protein interaction family proteins involved in the chloroplast movement response. Plant Signal Behav 6:483–490
La Notte L, Giordano L, Calabrò E, Bedini R, Colla G, Puglisi G, Reale A (2020) Hybrid and organic photovoltaics for greenhouse applications. Appl Energy 278:115582
Li Q, Kubota C (2009) Effects of supplemental light quality on growth and phytochemicals of baby-leaf lettuce. Environ Exp Bot 67:59–64
Li L, Wang H (2022) Editorial: Shade avoidance syndrome in plants. Front Plant Sci 13:990982
Li N, Gügel IL, Giavalisco P, Zeisler V, Schreiber L, Soll J, Philippar K (2015) FAX1, a novel membrane protein mediating plastid fatty-acid export. PLoS Biol 13:e1002053
Liu B, Zhao S, Li P, Yin Y, Niu Q, Yan J, Huang D (2021) Plant buffering against high-light stress-induced accumulation of CsGA2ox8 transcripts via alternative splicing to tune gibberellin levels and maintain hypocotyl elongation. Hortic Res 8:(article ID).
Loi M, Villani A, Paciolla F, Mulè G, Paciolla C (2020) Challenges and opportunities of LEDs as key to modulate antioxidant compounds in plants: a review. Antioxidants 10:42
Love MI, Anders S, Huber W (2014) Differential analysis of count data—the DESeq2 package. Genome Biol 15:550

Lu L, Ya'acob ME, Anuar MS, Mohtar MN (2022) Comprehensive review on inorganic and organic photovoltaics as greenhouse shading materials. Sustain Energy Technol Assess 52:102077

LuY,Chen M, Zhu G, Zhang Y (2024) Recent progress in integrated solar-cell–energy-storage systems. Nanoscale P 16:8778. https://doi.org/10.1039/d4nr00839a

Luccioni LG, Oliverio KA, Yanovsky MJ, Boccalandro HE, Casal JJ (2002) Brassinosteroid mutants uncover fine tuning of phytochrome signalling. Plant Physiol 128:173–181

Marrs KA (1996) The functions and regulation of glutathione S-transferases in plants. Annu Rev Plant Physiol Plant Mol Biol 47:127–158

Martínez-García JF, Galstyan A, Salla-Martret M, Cifuentes-Esquivel N, Gallemí M, Bou-Torrent J (2010) Regulatory components of shade-avoidance syndrome. Adv Bot Res 53:65–116

Mazzeo D, Di Zio A, Pesenti C, Leva S (2025) Optimizing agrivoltaic systems: A comprehensive analysis of design, crop productivity and energy performance in open-field configurations. Appl Energy 390:125750

Menicucci F, Marino G, Sillo F, Carli A, dos Santos Nascimento LB, Detti C et al (2025) Blue and red LEDs modulate polyphenol production in Precoce and Tardiva cultivars of *Cichorium intybus* L. Front Plant Sci 16:1529804

Mobini SH, Lulsdorf M, Warkentin TD, Vandenberg A (2016) Low red: far-red light ratio causes faster *in vitro* flowering in lentil. Can J Plant Sci 96:908–918

Montes-Romero J, Cruz-Escabias A, Almonacid F, Fernández EF (2025) Comparative analysis of semi-transparent photovoltaic technologies for agrivoltaic applications. Renew Energy 256:124573

Muñoz-García AB, Benesperi I, Boschloo G, Concepción JJ, Delcamp JH, Gibson EA et al (2021) Dye-sensitized solar cells strike back. Chem Soc Rev 50:12450–12550

Ntinas GK, Kadoglidou K, Tsivelika N, Krommydas K, Kalivas A, Ralli P, Irakli M (2019) Performance and hydroponic tomato crop quality in a greenhouse using dye-sensitized solar-cell covering. Horticulturae 5:42

Oshima Y, Mitsuda N (2013) The MIXTA-like transcription factor MYB16 is a major regulator of cuticle formation in vegetative organs. Plant Signal Behav 8:e26826

Park S, Kim J, Oh W (2024) Growth and leaf colour of coleus under light conditions modified by translucent agrivoltaic panels and LEDs in a greenhouse. Horticulturae 10:115

Pastor-Andreu P, Moreno-Romero J, Urdin-Bravo M, Palau-Rodriguez J, Paulisic S, Kastanaki E et al (2024) Temporal and spatial frameworks supporting plant responses to vegetation proximity. Plant Physiol 196:2048–2063

Pierik R, Cuppens ML, Voesenek LA, Visser EJ (2004) Interactions between ethylene and gibberellins in phytochrome-mediated shade-avoidance responses in tobacco. Plant Physiol 136:2928–2936

Pons TL, de Jong-Van Berkel YE (2004) Species-specific variation in the spectral-quality gradient in canopies as a signal for photosynthetic resource partitioning. Ann Bot 94:725–732

Poorter H, Niklas KJ, Reich PB, Oleksyn J, Poot P, Mommer L (2012) Biomass allocation to leaves, stems and roots: meta-analyses of interspecific variation and environmental control. New Phytol 193:30–50

Qin J, Duan W, Zou S, Chen Y, Huang W, Rosa L (2024) Global energy use and carbon emissions from irrigated agriculture. Nat Commun 15:3084

Reed JW, Nagpal P, Poole DS, Furuya M, Chory J (1993) Mutations in the gene for the red/far-red light receptor phytochrome B alter cell elongation and physiological responses throughout *Arabidopsis* development. Plant Cell 5:147–157

Reyt G, Chao Z, Flis P, Salas-González I, Castrillo G, Chao DY, Salt DE (2020) Uclacyanin proteins are required for lignified nanodomain formation within Casparian strips. Curr Biol 30:4103–4111e6

Roig-Villanova I, Martínez-García JF (2024) Molecular regulation of plant responses to shade. In: Lüttge U, Cánovas FM, Risueño M-C, Leuschner C, Pretzsch H (eds) Progress in Botany, vol 84. Springer, Cham, pp 221–240

Roppolo D, De Rybel B, Tendon VD, Pfister A, Alassimone J, Vermeer JE et al (2011) A novel protein family mediates Casparian strip formation in the endodermis. Nature 473:380–383

Roslan N, Ya'acob ME, Jamaludin D, Hashimoto Y, Othman MH, Iskandar AN et al (2021) Dye-sensitized solar cells: effects on light quality, microclimate and growth of *Orthosiphon stamineus*. Agronomy 11:631

Runkle ES, Heins RD (2001) Specific functions of red, far-red and blue light in flowering and stem extension of long-day plants. J Am Soc Hortic Sci 126:275–282

Schrager-Lavelle A, Herrera LA, Maloof JN (2016) Tomato phyE is required for shade avoidance in the absence of phyB1 and phyB2. Front Plant Sci 7:1275

Schwacke R, Ponce-Soto GY, Krause K, Bolger AM, Arsova B, Hallab A et al (2019) MapMan4: a refined protein classification and annotation framework for multi-omics data analysis. Mol Plant 12:879–892

Semeraro T, Scarano A, Curci LM, Leggieri A, Lenucci M, Basset A et al (2024) Shading effects in agrivoltaic systems can make the difference in boosting food security in climate change. Appl Energy 358:122565

Shcherban TY, Shi J, Durachko DM, Guiltinan MJ, McQueen-Mason SJ, Shieh M, Cosgrove DJ (1995) Molecular cloning and sequence analysis of expansins—a highly conserved, multigene family of proteins that mediate cell wall extension in plants. Proc Natl Acad Sci USA 92:9245–9249

Sheng C, Shi Y, Li Y, Wang W, Zhou W, Chen C et al (2025) Semi-transparent coloured solar cells for agrivoltaic ecosystem applications. Adv Sustain Syst 9:2401059

Sng BJR, Singh GP, Van Vu K, Chua NH, Ram RJ, Jang IC (2020) Rapid metabolite response in leaf blade and petiole as a marker for shade-avoidance syndrome. Plant Methods 16:144

Soussi A, Zero E, Ouammi A, Zejli D, Zahmoun S, Sacile R (2025) Smart greenhouse farming: a review towards near-zero energy consumption. Discover Cities 2:55

Spampinato C, Valastro S, Calogero G, Smecca E, Mannino G, Arena V et al (2025) Improved radicchio seedling growth under $CsPbI_3$ perovskite rooftop in a laboratory-scale greenhouse for agrivoltaics. Nat Commun 16:2190

Stallknecht EJ, Herrera CK, Yang C, King I, Sharkey TD, Lunt RR, Runkle ES (2023) Designing plant-transparent agrivoltaics. Sci Rep 13:1903

Stamford JD, Stevens J, Mullineaux PM, Lawson T (2023) LED lighting: a grower's guide to light spectra. HortScience 58:180–196

Stathatos E (2005) Organic–inorganic nanocomposite materials prepared by the sol-gel route as new ionic conductors in quasi solid-state electrolytes. Ionics 11:140–145

Stathatos E, Lianos P, Stangar UL, Orel B, Judeinstein P (2000) Structural study of hybrid organic/inorganic polymer gels using time-resolved fluorescence probing. Langmuir 16:8672–8676

Tang YJ, Liesche J (2017) The molecular mechanism of shade avoidance in crops: how data from *Arabidopsis* can help to identify targets for increasing yield and biomass production. J Integr Agric 16:1244–1255

Todd J, Post-Beittenmiller D, Jaworski JG (1999) KCS1 encodes a fatty acid elongase 3-ketoacyl-CoA synthase affecting wax biosynthesis in *Arabidopsis thaliana*. Plant J 17:119–130

Toledo-Ortiz G, Johansson H, Lee KP, Bou-Torrent J, Stewart K, Steel G et al (2014) The HY5–PIF regulatory module coordinates light

and temperature control of photosynthetic gene transcription. PLoS Genet 10:e1004416

Trépanier MP, Gosselin L, Jørgensen BN (2025) Optimal combinations of energy-efficiency measures in greenhouses considering energy consumption, yield and costs: comparison between two cold-climate cities. Appl Energy 382:125163

Ursu D, Vajda M, Miclau M (2022) Highly efficient dye-sensitized solar cells for wavelength-selective greenhouse applications: a promising agrivoltaic system. Int J Energy Res 46:18550–18561

Van Brenk JB, Courbier S, Kleijweg CL, Verdonk JC, Marcelis LF (2024) Paradise by the far-red light: far-red and red:blue ratios independently affect yield, pigments and carbohydrate production in lettuce. Front Plant Sci 15:1383100

Vandenbussche F, Vriezen WH, Smalle J, Laarhoven LJ, Harren FJ, Van der Straeten D (2003) Ethylene and auxin control the *Arabidopsis* response to decreased light intensity. Plant Physiol 133:517–527

Vandenbussche F, Pierik R, Millenaar FF, Voesenek LA, Van der Straeten D (2005) Reaching out of the shade. Curr Opin Plant Biol 8:462–468

Vo Phan MS, Keren I, Tran PT, Lapidot M, Citovsky V (2023) *Arabidopsis* LSH10 transcription factor and OTLD1 histone deubiquitinase interact and regulate the same target genes. Commun Biol 6:58

Wille W, Pipper CB, Rosenqvist E, Andersen SB, Weiner J (2017) Reducing shade-avoidance responses in a cereal crop. AoB Plants 9:plx039

Xia J, Mattson N (2024) Daily light integral and far-red radiation influence morphology and quality of liners and subsequent flowering and development of petunia in controlled greenhouses. Horticulturae 10:1106

Yu L, Zhou C, Fan J, Shanklin J, Xu C (2021) Mechanisms and functions of membrane lipid remodeling in plants. Plant J 107:37–53

Zhao Q, Nakashima J, Chen F, Yin Y, Fu C, Yun J et al (2013) Laccase is necessary and non-redundant with peroxidase for lignin polymerization during vascular development in Arabidopsis. Plant Cell 25:3976–3987

Zhu W, Gao E, Shaban M, Wang Y, Wang H, Nie X, Zhu L (2018) GhUMC1, a blue copper-binding protein, regulates lignin synthesis and cotton immune response. Biochem Biophys Res Commun 504:75–81

Publisher's Note Springer Nature remains neutral with regard to jurisdictional claims in published maps and institutional affiliations.